ORIGINAL PAPER

LiNi$_{0.8}$Co$_{0.2-x}$Ti$_x$O$_2$ nanoparticles: synthesis, structure, and evaluation of electrochemical properties for lithium ion cell application

R. Sathiyamoorthi · P. Santhosh · P. Shakkthivel · T. Vasudevan

Abstract Layered Ti-doped lithiated nickel cobaltate, LiNi$_{0.8}$Co$_{0.2-x}$Ti$_x$O$_2$ (where x=0.01, 0.03, and 0.05) nanopowders were prepared by wet-chemistry technique. The structural properties of synthesized materials were characterized by X-ray diffraction (XRD) and thermo-gravimetric/differential thermal analysis (TG/DTA). The morphological changes brought about by the changes in composition of LiNi$_{0.8}$Co$_{0.2-x}$Ti$_x$O$_2$ particles were examined through surface examination techniques such as scanning electron microscopy (SEM) and transmission electron microscopy (TEM) analyses. Electrochemical studies were carried out using 2016-type coin cell in the voltage range of 3.0–4.5 V (vs carbon) using 1 M LiClO$_4$ in ethylene carbonate and diethyl carbonate as the electrolyte. Among the various concentrations of Ti-doped lithiated nickel cobaltate materials, C/LiNi$_{0.8}$Co$_{0.17}$Ti$_{0.03}$O$_2$ cell gives stable charge–discharge features.

Introduction

In recent years, much attention has been given for the development of chemical and electrochemical reactions of lithium ion batteries [1, 2]. Layered structure transition metal oxides, such as LiCoO$_2$, LiNiO$_2$, and LiMnO$_2$ have been investigated extensively as the potential cathode materials for lithium ion batteries [3–12]. The main goal of most of the research is to develop non-toxic and cost-effective cathode materials to replace the existing high cost

and toxic LiCoO$_2$ cathode material, which is the cathode material for most of the commercial lithium ion batteries.

Among the various oxides used, LiNiO$_2$ is cheap and has higher energy density and, thus, aroused significant interests in recent years. However, it has been assumed that LiNiO$_2$ is not competent as a candidate for cathode material because of its shortcomings [5–11]. Doped LiNiO$_2$ compounds, such as LiNi$_{1-y}$Co$_y$O$_2$, are then considered as new candidates to replace LiCoO$_2$. Many studies on the LiNi$_{1-y}$Co$_y$O$_2$ compounds have provided better results [13–21]. The Co substitution for Ni stabilizes the two-dimensional layered structure and decreases the initial capacity loss and, thus, increases the cycle life of batteries.

Nevertheless, these studies have also demonstrated that LiNi$_{1-y}$Co$_y$O$_2$ materials are yet not able to improve the thermal stability at charged state, which is a key issue of safety consideration for lithium ion batteries. The introduction of other doping metal such as Al, Mn, Mg, Fe, Y, and Sr improve the cycle performance and thermal stability of the LiNi$_{1-y}$Co$_y$O$_2$ materials [22–28]. Tetravalent titanium (Ti^{4+}) was also used to substitute Ni for improving the properties of LiNiO$_2$. The LiNi$_{1-x}$Ti$_x$O$_2$ [29, 30], LiTi$_x$Co$_{1-x}$O$_2$ [31], and LiNi$_{1-x}$Ti$_{x/2}$Mg$_{x/2}$O$_2$ [32] materials have been reported with good electrochemical properties and thermal stability. More recently, LiNi$_{0.8}$Co$_{0.1}$Ti$_{0.1}$O$_2$ [33], LiNi$_{0.8}$Co$_{0.2-2y}$Ti$_y$Mg$_y$O$_2$ [34], and LiNi$_{0.7}$Co$_{0.2}$Ti$_{0.05}$Mg$_{0.05}$O$_2$ [35] were also reported with improved cycling performance and enhanced thermal stability. Hence, it seems that the tetravalent titanium has shown beneficial effect on the properties of layered structure, LiNiO$_2$-based materials. In this work, tetravalent titanium was introduced into LiNi$_{0.8}$Co$_{0.2}$O$_2$ compound as a substitute for Co through a sol–gel route, which allows a better mixing of the reactants at atomic level and produces highly homogeneous materials. The effect of titanium substitution on the structural, electro-

R. Sathiyamoorthi · P. Santhosh · P. Shakkthivel · T. Vasudevan (✉)
Department of Industrial Chemistry, Alagappa University, Karaikudi 630 003 Tamil Nadu, India
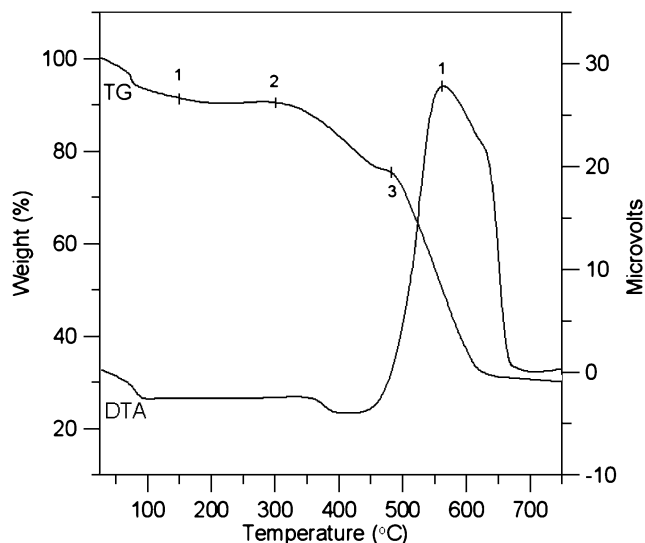e-mail: drtvasudevan2002@yahoo.com

Fig. 1 TG/DTA curves of $LiNi_{0.8}Co_{0.17}Ti_{0.03}O_2$

Table 1 XRD lattice parameters a and c (Å), and intensity ratios of 003 and 104 peaks (I) for $LiNi_{0.8}Co_{0.2-x}Ti_xO_2$

x	a	c	c/a	$I(003)/I(104)$
0	2.8492	14.021	4.9210	1.64
0.01	2.8579	14.049	4.9158	1.51
0.03	2.8623	14.060	4.9121	1.71
0.05	2.8657	14.069	4.9094	1.31

chemical, and thermal properties of $LiNi_{0.8}Co_{0.2-x}Ti_xO_2$ compounds were studied in detail.

Experimental

Solid precursor of $LiNi_{0.8}Co_{0.2-x}Ti_xO_2$ ($x=0$, 0.01, 0.03, and 0.05) compounds were obtained by sol–gel route from stoichiometric amounts of $Ni(NO_3)_2$, TiO_2, and $Co(NO_3)_2$, and 10% excess $LiNO_3$ solution in 4:1 citric acid/ethylene glycol mixture [36]. To get nitrate of titanium, we used a few drops of HNO_3 to the TiO_2 substance. A transparent green solution was formed. The mixture was stirred at 80 °C for 2 h. A dark-green gel was formed. Further, the gel was heated at 120 °C for 4 h to form a dry gel, which was calcined at 600 °C for 6 h in the muffle furnace. The reaction products were ground well into fine powder.
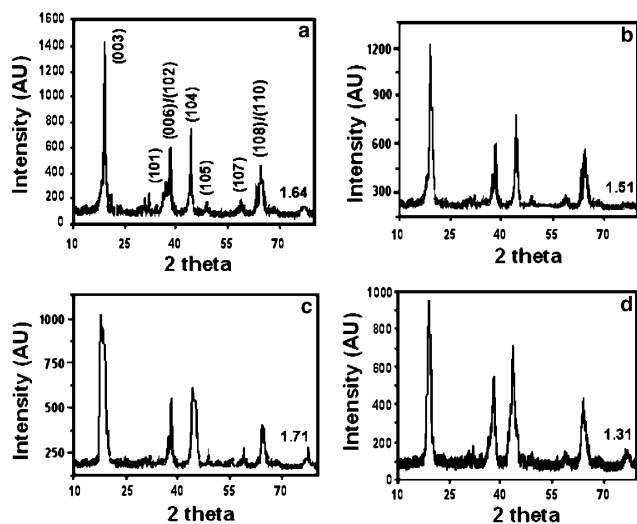
The synthesized samples were characterized by powder X-ray diffraction (XRD), using Joel model JDX-8D X-ray diffractometer. Data were collected in the range 10–80° using a step size of 0.02° and a counting time of 2 s per step. The refinements of unit cell parameters were carried out by least-square method. The morphology of the synthesized cathode materials was studied by both scanning electron microscope (SEM) Joel model 5600 LV and transmission electron microscope (TEM) Joel JEM-2000 EX.

The electrochemical behavior of the synthesized samples was tested using 2016-type coin cell. The 10-mm diameter electrodes were prepared as pellets by pressing a mixture of 85% of the active material mixed with 10% acetylene black and 5% poly(vinylidene fluoride) dissolved in N-methyl 2-pyrrolidinone (NMP) as the solvent; a 5-ton pressure was applied using hydraulic press for the electrode preparation. The commercial electrolyte solution (Aldrich, 1 M $LiClO_4$ in a 1:1 v/v mixture of ethylene carbonate, diethyl carbonate) and polypropylene separator were used. The electrochemical experiments were carried out using a WonA Tech, potentiostat/galvanostat 100 system in the voltage range of 3.0–4.5 V at a constant current density of 0.1 mA/cm².
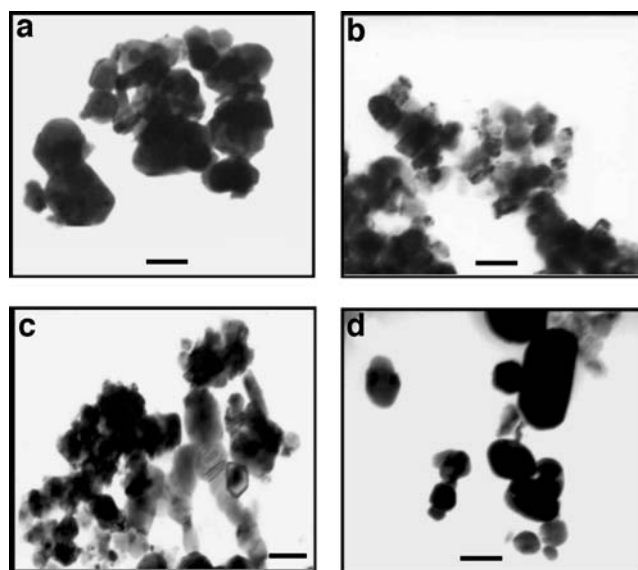

Fig. 2 XRD patterns of $LiNi_{0.8}Co_{0.2-x}Ti_xO_2$ cathode materials. $x=0$ (**a**), 0.01 (**b**), 0.03 (**c**), and 0.05 (**d**). The peak intensity ratio $I(003)/I(104)$ was also presented at the right of the graph for comparison

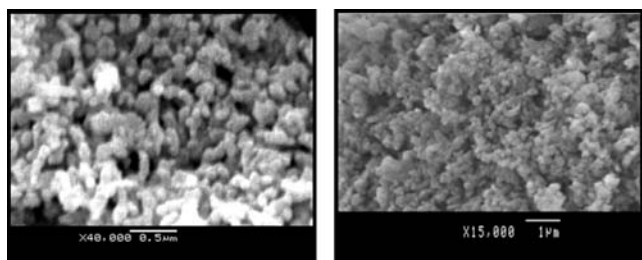**Fig. 3** TEM images of $LiNi_{0.8}Co_{0.2-x}Ti_xO_2$. $x=0$ (**a**), 0.01 (**b**), 0.03 (**c**), and 0.05 (**d**); scale bar, 100 nm

Fig. 4 SEM images of $LiNi_{0.8}Co_{0.17}Ti_{0.03}O_2$ under different magnifications

Results and discussion

Structural studies

The thermo-gravimetric/differential thermal analysis (TG/DTA) curves of the $LiNi_{0.8}Co_{0.2-x}Ti_xO_2$ precursor ($x=0.03$) are shown in Fig. 1; a 10% weight loss occurs initially until 150 °C and an additional decrease of 10% is observed at 400 °C. The initial decrease is due to the thermal decomposition of solvent, nitrate, and ammonia, and the further weight loss is due to the thermal decomposition of the citric acid and ethylene glycol into C and O_2. No weight loss is observed above 600 °C.

The XRD patterns of all the $LiNi_{0.8}Co_{0.2-x}Ti_xO_2$ samples ($x \leq 0.05$) obtained in this work could be ascribed to the layered products. Figure 2 shows the XRD patterns of all samples calcined at 600 °C for 6 h, in which the R3-m space group reflections have been indexed. It is observed from the X-ray patterns that the entire fingerprint peaks, viz. 003, 101, 006, 102, 104, 108, and 110, are clearly identifiable, thereby, suggesting the formation of the α-$NaFeO_2$ structure. The diffraction peaks of the synthesized $LiNi_{0.8}Co_{0.2}O_2$ are in agreement with the literature [37]. With the increase of titanium, the full-width half maximum (FWHM) of the peaks broadens and the peak intensity decreases, which indicates
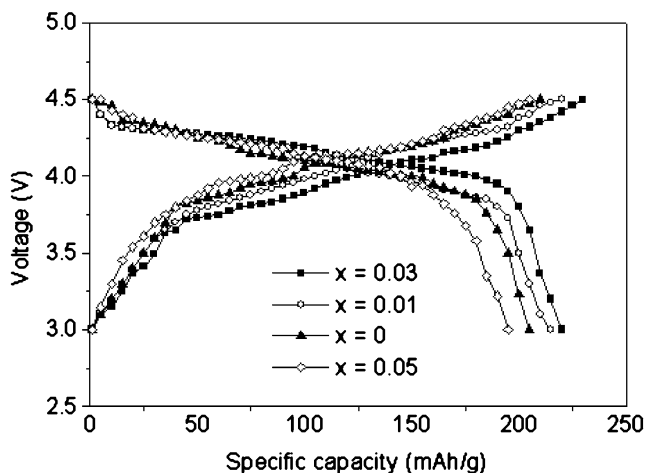
Table 2 Charge-discharge data for $LiNi_{0.8}Co_{0.2-x}Ti_xO_2$ cathode materials

Sample	First cycle			25th cycle	Capacity retention (%)
	Q_{charge} (mAh/g)	$Q_{discharge}$ (mAh/g)	Loss (%)		
$x=0$	210	187	11	140	74
$x=0.01$	219	195	11	157	80
$x=0.03$	230	206	10	171	83
$x=0.05$	205	170	17	112	65

that the crystallization is weakened for the titanium-doped materials. XRD patterns of the samples show reflections close to $\theta=30$. These reflections are likely to arise from the spinel phase of Co_3O_4. It is found that the $I(003)/I(104)$ peak intensity ratio shows a decreasing tendency with an increase of titanium amount from 1.64 for $x=0$ to 1.31 for $x=0.05$. However, a higher ratio value of about 1.71 is observed for $x=0.03$. The degree of either (108)/(110) or (006)/(102) peak splitting changes from clear to indistinct with an increase of x value, as the two characters of XRD patterns, i.e., $I(003)/I(104)$ ratio and (108)/(110) or (006)/(102) peak splitting, were considered the evidence for the degree of ordering layered structure, as well as the amount of transition metal in the inter-slab space [38, 39]. This implies that the titanium substitution for cobalt in $LiNi_{0.8}Co_{0.2-x}Ti_xO_2$ compounds has affected the cationic distribution and the crystal structure. Because excess lithium nitrate was provided to compensate lithium loss, the Bragg intensity ratio $R(003)=I(003)/I(104)$ shows a relatively high value of 1.3–2.5. This value can serve as a quantitative interior for the stoichiometry and degree of order in this $LiCoO_2$ system. The data in Table 1 can be used to determine how the hexagonal cell parameters vary with x in $LiNi_{0.8}Co_{0.2-x}Ti_xO_2$ compounds. As the
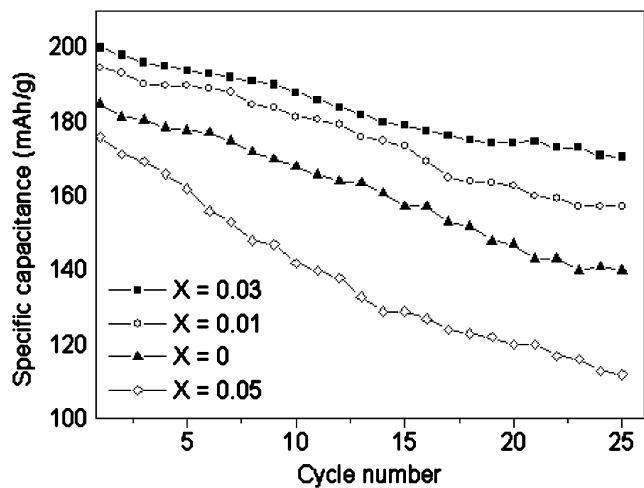

Fig. 5 The first charge–discharge curves of $LiNi_{0.8}Co_{0.2-x}Ti_xO_2$ ($x=0$, 0.01, 0.03, and 0.05) cathode materials at a current rate of 0.1 mA/cm^2 in a voltage range of 3.0–4.5 V

Fig. 6 Plots of discharge-specific capacity vs the cycle no. for $LiNi_{0.8}Co_{0.2-x}Ti_xO_2$ ($x=0$, 0.01, 0.03, and 0.05) cathode materials at a current rate of 0.1 mA/cm^2 in a voltage range of 3.0–4.5 V

amount of titanium increases, both the average metal–metal intra-sheet distance (a_{hex}) and the average metal–metal interlayer distance (c_{hex}) increases. The degree of trigonal distortion (c/a) of the $LiNi_{0.8}Co_{0.2-x}Ti_xO_2$ samples is typical of hexagonal close-packed structure (4.90–4.95).

TEM images of $LiNi_{0.8}Co_{0.2-x}Ti_xO_2$ ($x=0$, 0.01, 0.03, and 0.05) are presented in Fig. 3. The particles show good morphology with uniform distribution (~50 nm) of sizes. Representative SEM image for $LiNi_{0.8}Co_{0.17}Ti_{0.03}O_2$ is presented in Fig. 4. The particles are found to be crystalline with well-defined facets. Further, the particles exhibit a uniform distribution and are smaller than the parent $LiNi_{0.8}Co_{0.2}O_2$ compounds [37].

Electrochemical charge–discharge features

The charge–discharge electrochemical properties of $LiNi_{0.8}Co_{0.2-x}Ti_xO_2$ ($x=0$, 0.01, 0.03, and 0.05) compounds were tested galvanostatically at a constant current density of 0.1 mA/cm^2 between 3.0 and 4.5 V. The first charge–discharge cycling curves for the $LiNi_{0.8}Co_{0.2-x}Ti_xO_2$ ($x=0$, 0.01, 0.03, and 0.05) systems are shown in Fig. 5. The first discharge capacity of $LiNi_{0.8}Co_{0.2}O_2$ is as high as 187 mAh/g and stabilizes after few cycles at 155 mAh/g. The average capacity is 160 mAh/g, which is comparable with values reported in the literature [37]. A part of the discharge data for $LiNi_{0.8}Co_{0.2-x}Ti_xO_2$ cathode materials is presented in Table 2. It can be seen that an increase in charge-specific capacity with an increase of doped titanium amount from 210 mAh/g ($x=0$) to 230 mAh/g ($x=0.03$). Discharge-specific capacity increases to 206 mAh/g ($x=0.03$) from 187 mAh/g ($x=0$). A raised charge voltage plateau with the increasing amount of titanium is observed (Fig. 5); however, at the highest concentration of Ti ($x=0.05$), drastic fall in capacity is observed. Reasonable capacity loss occurred commonly in all the cathode materials after the first cycle and shows almost retrieved thereafter. This is attributed to the improved structure stability during cycling. The decrease of the capacity losses is originated from the lattice changes, and interface reactions compensate the increase of the capacity losses, which is caused by the extra transition metal at the $3a$ Li site. The results infer that the initial capacity loss of $LiNi_{0.8}Co_{0.2-x}Ti_xO_2$ cathodes is not significant when compared with the $LiNi_{0.8}Co_{0.2}O_2$ cathode.

The cycle life curves for $LiNi_{0.8}Co_{0.2-x}Ti_xO_2$ cathode materials were recorded at 0.1 mA/cm^2 constant current rates for 25 cycles in the voltage range of 3.0–4.5 V (Fig. 6). It is clear that the Ti substitution improves the cycle stability of the cathode materials, although there is slight capacity fading in all the cycles. The discharge capacity of $LiNi_{0.8}Co_{0.2}O_2$ cathode decreases from 187 to 140 mAh/g after 25 cycles with a capacity retention of 74%. It seems that the capacity retention of $LiNi_{0.8}Co_{0.2}O_2$

is slightly different from previous reports, which may be attributed to the differences in sample synthesis and electrode preparation. However, for $LiNi_{0.8}Co_{0.17}Ti_{0.03}O_2$ cathode, discharge capacity fades from 206 to 171 mAh/g only after 25 cycles with a high capacity retention of 83%.

Conclusions

Layered Ti-doped lithiated nickel cobaltate, $LiNi_{0.8}Co_{0.2-x}Ti_xO_2$ (where $x=0.01$, 0.03, and 0.05) nanopowders were prepared by wet-chemistry technique. XRD studies shows that the titanium is incorporated into the $LiNi_{0.8}Co_{0.2-x}Ti_xO_2$ ($x \leq 0.03$) solid solutions, and the hexagonal close-packed unit cell parameters increases with the substitution of cobalt by titanium. The substitution of very small amounts of cobalt by titanium in $LiNi_{0.8}Co_{0.2}O_2$ leads to a net improvement of the reversible capacity and capacity retention in lithium cells. Changes in the electrochemical performance were correlated with X-ray line broadening analysis, which reveals that the increase of crystallinity increases the cell capacity. Therefore, it can be concluded that the titanium substitution for cobalt has a good beneficial effect on the cycle performance and thermal stability of $LiNi_{0.8}Co_{0.2}O_2$ material.

References

1. Scrosati B (1993) Nature 373:557
2. Lave LB, Hendrickson CT, Mcmichael FC (1993) Science 268:993
3. Mizushima K, Jone PC, Wiseman, Goodenough JB (1980) Mater Res Bull 15:783
4. Reimers JN, Dahn JR (1992) J Electrochem Soc 139:2091
5. Thomas MGSR, David WIF, Goodenough JB, Groves P (1985) Mater Res Bull 20:1137
6. Morales J, Vicente CP, Tirado JT (1990) Mater Res Bull 25:623
7. Li W, Reimers JN, Dahn JR (1993) Solid State Ion 67:123
8. Ohzuku T, Ueda A, Nagayama M (1993) J Electrochem Soc 140:1862
9. Peres JP, Delmas C, Rougier A, Broussely M, Perton F, Piensan P, Willmann P (1996) J Phys Chem Solids 57:1057
10. Rougier A, Gravereau P, Delmas C (1996) J Electrochem Soc 143:1168
11. Arai H, Okada S, Sakurai Y, Yamaki J (1998) Solid State Ion 109:29
12. Armstrong AR, Bruce PG (1996) Nature 381:499
13. Ohzuku T, Lomori H, Swai L, Hirai T (1990) Chem Express 5:733
14. Delmas C, Saadoune I (1992) Solid State Ion 53:370
15. Gummow RJ, Thackeray MM (1993) J Electrochem Soc 140:3365
16. Ueda A, Ohzuku T (1994) J Electrochem Soc 141:2010
17. Saadoune I, Delmas C (1996) J Mater Chem 6:193
18. Li W, Currie JC (1997) J Electrochem Soc 144:2773

19. Saadoune I, Delmas C (1998) J Solid State Chem 136:8
20. Lee KK, Kim KB (2000) J Electrochem Soc 147:1709
21. Chebiam RV, Prado F, Manthiram A (2001) J Electrochem Soc 148:A49
22. Chang CC, Kim JY, Kim PN (2000) J Power Sources 89:56
23. Yoshio M, Noguchi H, Itoh J, Okada M, Mouri T (2000) J Power Sources 90:176
24. Madhavi S, Rao GVS, Chowdari BVR, Li SFY (2001) J Power Sources 93:156
25. Prado G, Fournes L, Delmas C (2001) J Solid State Chem 159:103
26. Depifanio A, Croce G, Ronci F, Albertini VR Traversa E, Scrosati B (2001) Phys Chem Chem Phys 3:4399
27. Park SH, Park KS, Sun YK, Nahm KS, Lee YS, Yoshio M (2001) Electrochim Acta 46:1215
28. Fey GTK, Subramanian V, Chen JG (2002) Mater Lett 52:197
29. Kim J, Amine K (2001) Electrochem Commun 3:52
30. Kim J, Amine K (2002) J Power Sources 104:33
31. Gopukumar S, Jeong Y, Kim KB (2003) Solid State Ion 59:223
32. Gao Y, Yokovleva MV, Ebner WB (1998) Electrochem Solid-State Lett 1:117
33. Arai H, Tsuda M, Sakurai Y (2000) J Power Sources 90:76
34. Chowdari BVR, Subba Rao GV, Chow SY (2001) Solid State Ion 140:55
35. Subramanian V, Fey GTK (2002) Solid State Ion 148:351
36. Alcantara R, Lavela P, Tirado JL, Stoyanova R, Kuzmanova E, Zhecheva E (1997) Chem Mater 9:2145
37. Gong ZL, Liu SH, Guo XJ, Zhang ZR, Yong Y (2004) J Power Sources 136:139
38. Li W, Reimers JN, Dahss JR (1993) Solid State Ion 67:123
39. Peres JP, Delmas C, Rougier A, Broussely M, Perton F, Biensan P, Willmann P (1996) J Phys Chem Solids 57:1057